2015-10-20

An invertebrate smooth muscle with striated muscle myosin filaments

Guidenn Sulbaran
University of Massachusetts Medical School

Et al.

An invertebrate smooth muscle with striated muscle myosin filaments

Guidenn Sulbarán[a,b,1], Lorenzo Alamo[a,1], Antonio Pinto[a], Gustavo Márquez[a], Franklin Méndez[a], Raúl Padrón[a,2], and Roger Craig[b,2]

[a]Centro de Biología Estructural, Instituto Venezolano de Investigaciones Científicas (IVIC), Caracas 1020A, Venezuela; and [b]Department of Cell and Developmental Biology, University of Massachusetts Medical School, Worcester, MA 01655

Edited by James A. Spudich, Stanford University School of Medicine, Stanford, CA, and approved September 10, 2015 (received for review July 13, 2015)

Muscle tissues are classically divided into two major types, depending on the presence or absence of striations. In striated muscles, the actin filaments are anchored at Z-lines and the myosin and actin filaments are in register, whereas in smooth muscles, the actin filaments are attached to dense bodies and the myosin and actin filaments are out of register. The structure of the filaments in smooth muscles is also different from that in striated muscles. Here we have studied the structure of myosin filaments from the smooth muscles of the human parasite *Schistosoma mansoni*. We find, surprisingly, that they are indistinguishable from those in an arthropod striated muscle. This structural similarity is supported by sequence comparison between the schistosome myosin II heavy chain and known striated muscle myosins. In contrast, the actin filaments of schistosomes are similar to those of smooth muscles, lacking troponin-dependent regulation. We conclude that schistosome muscles are hybrids, containing striated muscle-like myosin filaments and smooth muscle-like actin filaments in a smooth muscle architecture. This surprising finding has broad significance for understanding how muscles are built and how they evolved, and challenges the paradigm that smooth and striated muscles always have distinctly different components.

thick filament | muscle structure | muscle contraction | schistosome | *Schistosoma mansoni*

The muscles of animals are of two basic types: striated or smooth. The presence or absence of striations depends on whether or not the thick (myosin) and thin (actin) filaments are in longitudinal register (1). In striated muscles, thin filaments of similar lengths are aligned via their attachment to transversely arranged Z-lines, which form the boundaries of the contractile unit, called the sarcomere. Thick filaments, also of similar lengths and in register, lie midway between the Z-lines (1). The repeating pattern of sarcomeres joined end-to-end gives rise to the striations seen in the light microscope (2). Smooth muscles, in contrast, lack both Z-lines and aligned, uniform-length thick and thin filaments; striations are therefore absent, creating a "smooth" appearance in the light microscope. In these muscles the Z-lines are replaced by narrower dense bodies, which act as attachment sites for thin filaments (3). In most animals, striated muscles are specialized for rapid, precisely controlled movements, whereas smooth muscles are used for slow or sustained contraction (1, 3). Within these broad categories there is considerable diversity in structure and function across species. Thus, striated muscles may be cross-striated (vertebrates and invertebrates) or obliquely/helically striated (invertebrates only) (4, 5), and smooth muscles may have relatively short (vertebrates and many invertebrates) or very long (molluscan) myosin filaments (6).

Our knowledge of the molecular structure and function of smooth muscle, and how this contrasts with striated muscle, has come mostly from studies of vertebrates. Several key differences are found: (*i*) The striated muscle myosin II heavy chain (MHC II) has key sites of sequence conservation in the tail and head, which clearly distinguish it from smooth and nonmuscle myosin II sequences (7, 8). (*ii*) Striated muscles are regulated via Ca^{2+} binding to troponin on the thin filaments (9), whereas smooth muscles lack troponin and are regulated by Ca^{2+}-induced phosphorylation of the myosin regulatory light chains (10). (*iii*) The thick filaments in striated muscles have a helical, bipolar structure, in which the polarity of myosin molecules reverses midway along the filament length, whereas smooth muscle thick filaments are nonhelical and side-polar, with oppositely oriented myosin molecules on opposite sides of the filament along its entire length (11, 12). Whether comparable differences occur in invertebrate muscle has been little studied, with the exception of molluscan smooth muscles, which have giant thick filaments (containing high levels of paramyosin) that are specialized to function in the long-lived, high-tension "catch" state (13).

Here we have studied the molecular structure and function of the muscles of the parasitic flatworm *Schistosoma mansoni*, which is responsible for the tropical disease schistosomiasis, affecting 200 million people worldwide (14). Our interest in these muscles was catalyzed by reports that the drug used to treat schistosomiasis (praziquantel) may act on the myosin molecule (15), and that muscle proteins like myosin, paramyosin, and certain regions of actin might be useful targets for the development of an anti-schistosomal vaccine or chemotherapy (16–18). We show that the adult form of *S. mansoni* has exclusively smooth muscles, and yet its thick filaments have the bipolar, helical structure characteristic

Significance

All animals have the ability to move. In most animals, striated muscles move the body and smooth muscles the internal organs. In both muscles, contraction results from interaction between myosin and actin filaments. Based on vertebrate studies, smooth and striated muscles are thought to have different protein components and filament structures. We have studied muscle ultrastructure in the parasite *Schistosoma mansoni*, where we find that this view is not supported. This invertebrate possesses only smooth muscles, yet its myosin sequence and filament structure are identical to those of striated muscle, while its actin filaments are smooth muscle-like. Such "hybrid" muscles may be common in other invertebrates. This finding challenges the paradigm that smooth and striated muscles always have different components.

Author contributions: G.S., L.A., A.P., R.P., and R.C. designed research; G.S., L.A., A.P., G.M., F.M., R.P., and R.C. performed research; G.S., L.A., A.P., R.P., and R.C. analyzed data; and G.S., R.P., and R.C. wrote the paper.

The authors declare no conflict of interest.

This article is a PNAS Direct Submission.

Data deposition: The *Schistosoma mansoni* negatively stained thick filament 3D map has been deposited into the Electron Microscopy Data Bank, www.ebi.ac.uk/pdbe/emdb (EMD-6370), and the atomic coordinates of the rigid docked model of myosin II interacting heads have been deposited into the Research Collaboratory for Structural Bioinformatics (PDB ID code 3JAX).

[1]G.S. and L.A. contributed equally to this work.

[2]To whom correspondence may be addressed. Email: raul.padron@gmail.com or roger.craig@umassmed.edu.

This article contains supporting information online at www.pnas.org/lookup/suppl/doi:10.1073/pnas.1513439112/-/DCSupplemental.

of striated muscle filaments from other invertebrates. This similarity in thick filament structure is supported by sequence analysis, which groups the schistosome MHC II with other striated muscle myosin sequences, not with their smooth/non-muscle counterparts. Whereas the thick filaments of schistosome smooth muscles have striated muscle characteristics, their thin filaments appear to lack troponin and are not regulated by Ca^{2+}; they are thus similar to other smooth muscle thin filaments. We conclude that, in contrast to vertebrates, schistosome smooth muscles are hybrids, incorporating proteins and filament structures from both smooth and striated muscles.

Results

Muscle Ultrastructure. To determine the type of muscle present in *S. mansoni*, adult male and female worms were fixed and embedded for ultrathin sectioning. Sections were cut at ~1- to 3-mm intervals along their body length and examined by transmission electron microscopy (EM). In longitudinal view, all muscles showed a filament organization typical of smooth muscle. Thick and thin filaments were readily visible, but neither set of filaments was in register and there was no regular banding characteristic of striated muscle (Fig. 1 *A* and *B*). Z-lines were absent, and dense bodies were prominent but not aligned transversely with each other. This organization was confirmed in transverse section (Fig. 1*C*). Thick and thin filaments were readily visible, interspersed with amorphous dense bodies. No Z-line lattice was seen in any cross-section. We conclude that the body musculature of the adult schistosome, both male and female, is smooth muscle.

Thick Filament Structure. Thick filaments were isolated from adult schistosomes. The small size of these organisms (~10 mm in length and 1-mm diameter for the male, and 11 mm and 0.2 mm, respectively, for the female) precluded dissecting out individual muscles. Whole worms were therefore used. Approximately 6,000

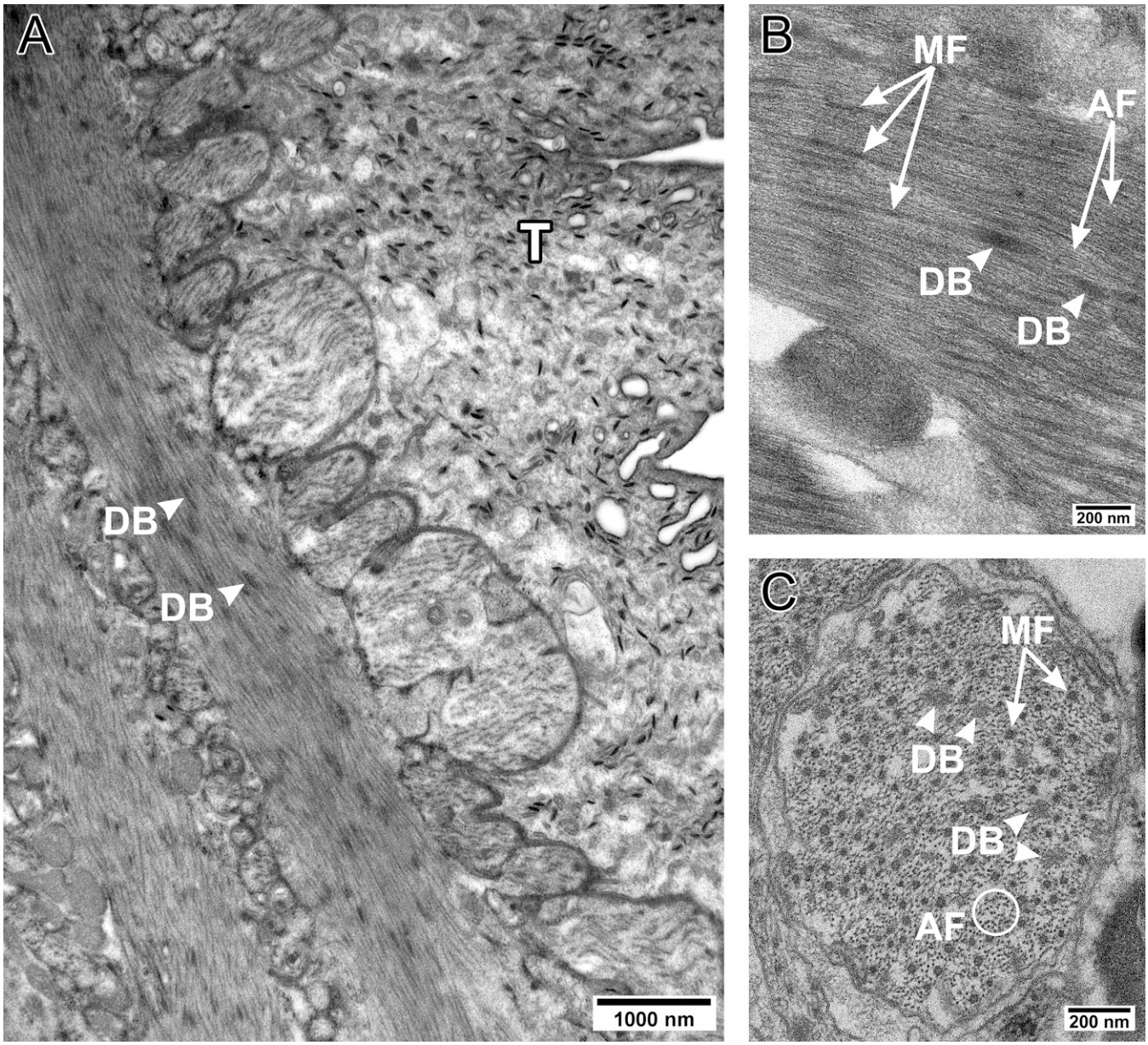

Fig. 1. Electron micrographs of adult schistosome muscle. (*A* and *B*) Longitudinal sections showing dense bodies (DB), myosin filaments (MF), actin filaments (AF), and absence of striations. T, Tegument. (*C*) Transverse section showing dense bodies, myosin filaments, and actin filaments.

worms, obtained from 15 to 20 hamsters, were detergent-skinned in relaxing medium and homogenized (*Materials and Methods*). The resulting filament suspension was examined by negative-staining EM and found to contain thin and thick filaments.

To our surprise, the thick filaments, which we have established above originate exclusively from smooth muscle, were indistinguishable from the striated muscle thick filaments of chelicerate arthropods (tarantula, scorpion, and *Limulus*) that we and others have studied previously (19–21). The myosin filaments of schistosome and arthropods also resembled each other in containing paramyosin (see, for example, Fig. 3). The filaments showed a clear bipolar structure with a central bare zone (Fig. 2*A*). Thick filament length was 3.6 ± 0.3 μm (mean ± SD) (n = 47); the diameter was 31.1 ± 2.8 nm (n = 967) in the head region and 22.2 ± 2.5 nm (n = 43) at the bare zone. The filaments displayed a regular pattern of myosin heads (Fig. 2*A*), similar to the helical organization seen in the chelicerates. Fourier transforms of individual filaments were essentially identical to those of the chelicerates (19–21), with a series of layer lines indexing on an ∼43.5-nm repeat, and meridional reflections at 14.5 and 7.2 nm (Fig. 2*B*). This finding confirms the helical symmetry of the filaments and their visual similarity to those of the chelicerates.

To understand the structure of these filaments in molecular detail, 3D reconstruction was carried out by single-particle methods. Consistent with the above findings, the reconstruction had an appearance essentially identical to that of the chelicerate striated muscle filaments (22–24). Four myosin molecules were present at each 14.5-nm "crown," each with a characteristic motif representing a pair of myosin heads (22) (Fig. 2 *C* and *D*). Atomic fitting of myosin head crystallographic structures into the reconstruction confirmed that this represented a pair of asymmetrically interacting myosin heads (Fig. 2*C*), as previously observed in the chelicerates (22). These interactions are thought to inhibit head activity in relaxed muscle by sterically blocking their actin-binding or ATPase sites (25). We conclude that the muscles of adult schistosomes, which are exclusively smooth, are nevertheless built from striated muscle-like thick filaments.

Myosin II Sequence. Invertebrate myosin II molecules have been classified as striated or nonmuscle (26), whereas vertebrate myosin

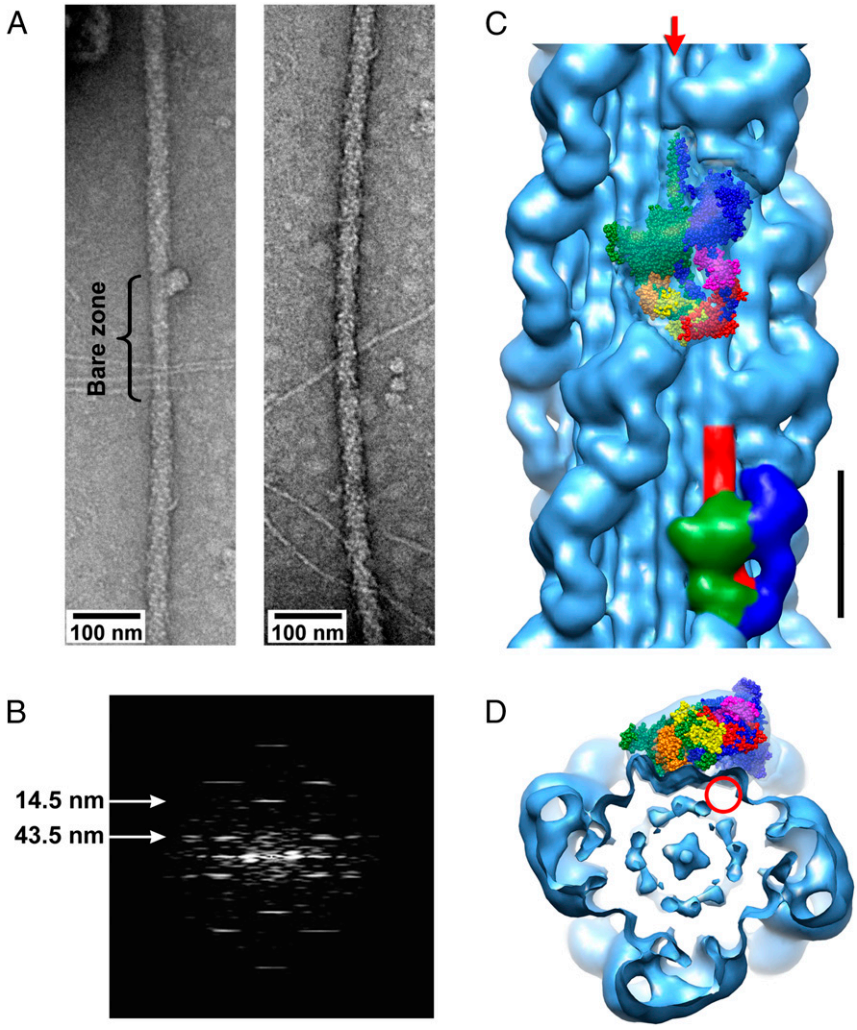

Fig. 2. Electron micrographs and 3D reconstruction of negatively stained *S. mansoni* thick filaments in relaxing conditions. (*A*) Thick filaments showing regularly ordered pattern of myosin heads (*Right*) and central "bare zone" (absence of heads) (*Left*). (*B*) Fourier transform of part of right filament in *A*, showing six orders of the 43.5-nm helical repeat of myosin heads. (*C* and *D*) Three-dimensional reconstruction of negatively stained thick filaments (EMD-6370) showing repeating motifs of paired myosin interacting-heads (bottom pair colored green and blue, with S2 red) in longitudinal view (*C*), and 12 subfilaments in transverse view (circle in *D*, arrow in *C*) (22). The repeating motifs, equally spaced around the filament circumference, form crowns at axial intervals of 14.5 nm, with fourfold rotational symmetry. *C* and *D* show fitting of atomic models of heavy meromyosin (PDB ID code 3JAX) into the motif (green and blue, MHC; orange and magenta, essential light chains; yellow and red, regulatory light chains) (50). (Scale bar for *C* and *D*, 14.5 nm).

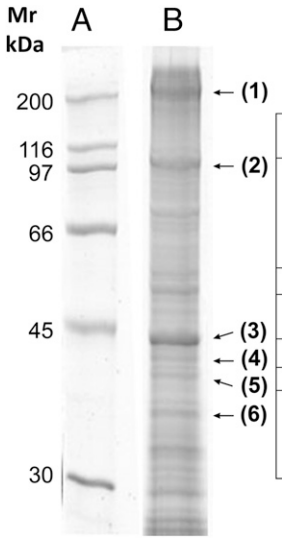

Protein	Peptide	Mascot Score	GeneBank Entry code
(1) Myosin Heavy Chain	FEDEQGLVAQLQR	54>49	gi|256086965
	FFLIEDMANLTHLNDASVLENL	53>47	
	NLSDEIHDLTEQLGEGG	113>49	
	LQGELEDLMVDVE	54>49	
	LEQDINELEVSLDGAN	96>62	
(2) Paramyosin	HAADLGFQVDALSER	82>23	gi|256074631
(3) Actin	QEYDESGPGIVHR	94>63	gi|256079407
	SYELPDGQVITIGNER	121>48	gi|256079405
(4) Tropomyosin 2	INQLEEQLKESTFMAEDADR	101>44	gi|256076631
(5) Troponin T	TVFTGANYAEEYQR	50<63	gi|256066240
(6) Tropomyosin 1	AVQYEELLK	70>53	gi|1174754
	ATNAEAEVAAMTR	70>53	
	LLEEDLEVSSSR	79>45	
	ALEISEQESAQREESYEETIR	108>44	

Fig. 3. SDS/PAGE and MS analysis of adult schistosome homogenate. Ten percent gel of (*A*) standard molecular weight markers and (*B*) *S. mansoni* homogenate. The numbers indicate the bands cut and analyzed by MS MALDI-TOF-TOF: number 1 was identified as *S. mansoni* MHC II (Uniprot entry Q02456), corresponding to a single MHC II gene (gi|256086965), based on the peptide sequences shown in the table; by sequence comparison this was deduced to be striated muscle type (Figs. 4 and 5). Other bands in the molecular weight regions corresponding to important sarcomeric proteins were also analyzed. Those found to be sarcomeric are labeled (arrows), whereas others found to be nonsarcomeric are not (Antigen Sm20, Antigen Sm14, Thioredoxin peroxidase, and so forth). The presence of tropomyosin and troponin T was confirmed in a 2D gel (Fig. S1). The lanes shown were selected and cropped from the original scanned gel. The MS analysis of ionized peptides obtained by MALDI-TOF-TOF is shown in the table on the right. Mascot was used as a search engine for protein identification (*Materials and Methods*). Only significant Mascot scores were considered for positive identification. According to the Mascot algorithm, the ion score for an MS/MS match is based on the calculated probability, P, that the observed match between the experimental data and the database sequence is a random event. The reported score is −10Log(P).

II also includes a smooth type similar in sequence to nonmuscle myosin (27, 28). The *S. mansoni* genome reveals multiple striated-type and nonmuscle MHC II genes (www.genedb.org/Homepage/Smansoni) (29). By proteomic analysis we detected significant expression, at the protein level, of only one myosin II isoform in adult *S. mansoni*: Q02456 (Fig. 3*B*). The average distance tree of aligned complete myosin II sequences shows clearly that this MHC II is of the striated muscle type, closer to striated MHC II of arthropods and molluscs than to that of vertebrates, but quite distinct from the smooth/nonmuscle MHC II group (Fig. 4). Separate alignment of the entire head and the entire tail gave the same result (cf. ref. 28). This striated vs. smooth/nonmuscle dichotomy was confirmed by

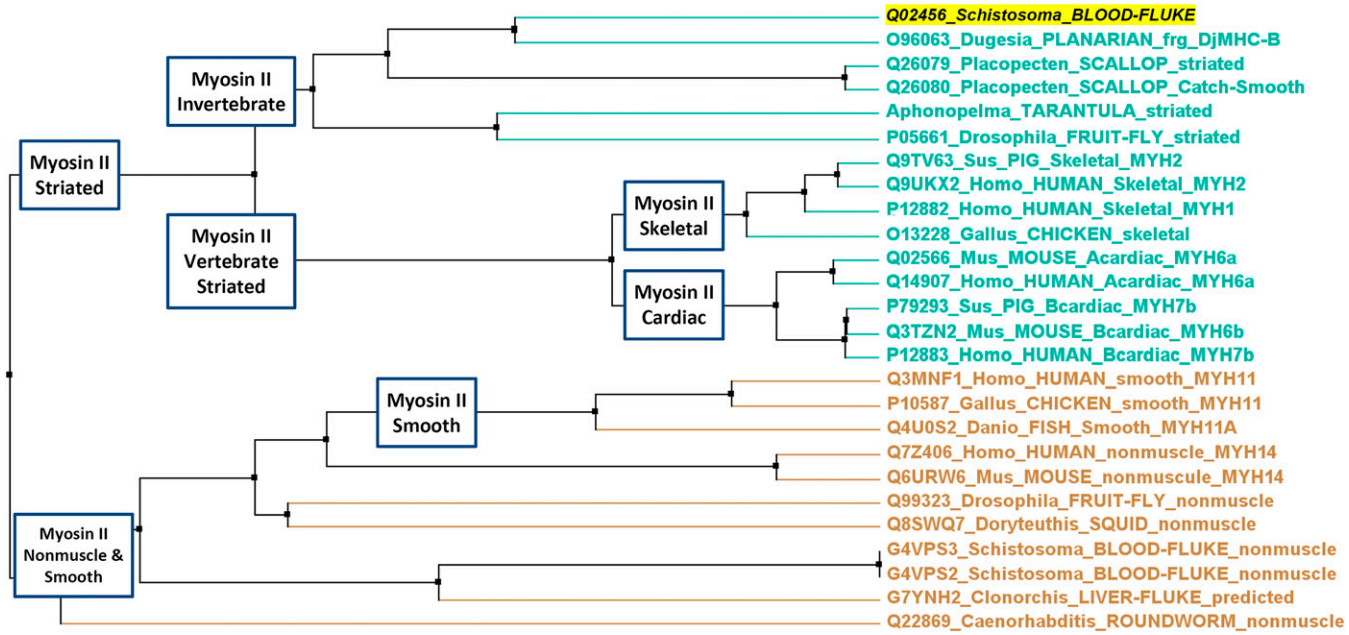

Fig. 4. Average distance tree for MHC II sequence alignment showing that MHC II is either striated- or smooth-like (cyan or tan, respectively). The schistosome MHC II (Q02456), highlighted in yellow was demonstrated to be present at the transcription level (80) and in the thick filament homogenate by proteomic analysis (Fig. 3); it was compared with complete sequences of the other myosins shown. The sequence segregates with striated muscle MHC IIs of vertebrates and invertebrates (cyan group), and not with smooth and nonmuscle myosins (tan group).

comparing four key regions previously associated specifically with striated MHC II: two actin binding regions (loops 2 and 3) (30), the IQ motif region (31), and a tail region defined as a striated muscle-specific site (7, 8) (Fig. 5). Finally, analysis of the MHC II tail sequence reveals that the schistosome has four skip residues in the α-helical coiled-coil, a feature in common with other striated muscle sequences (32–34) and different from the three skip residues characteristic of smooth/nonmuscle myosins. These multiple comparisons all lead to the same conclusion: that adult schistosome MHC II, which is derived exclusively from smooth muscle, is a striated-type myosin.

Regulation of Contraction. We used the in vitro motility assay as a functional test to determine whether schistosome smooth muscle is regulated through the thin filaments (as in most striated muscles) or the thick filaments (as in vertebrate smooth muscle). Thin filaments from a schistosome homogenate were labeled with fluorescent phalloidin and their motion over native tarantula striated muscle thick filaments was observed at different Ca^{2+} levels. Sliding occurred at both high (pCa < 4) and low (pCa > 9) calcium levels and had a similar velocity to F-actin (which is unregulated), indicating that schistosome thin filaments are not calcium-regulated (Table 1). This finding contrasts with similarly prepared thin filaments from tarantula striated muscle, known to contain troponin (35), whose sliding over both tarantula and schistosome thick filaments displayed clear Ca^{2+}-sensitivity (Table 2). The *S. mansoni* genome has genes for all components of the troponin–tropomyosin (Tn/Tm) complex except troponin C (TnC) (29), which is responsible for Ca^{2+} binding (9). Consistent with this, mass spectrometry revealed the expression of Tm (two isoforms), actin, troponin T (TnT) (Fig. 3), and troponin I (TnI) (Fig. S1) in the adult muscle homogenate (Fig. 3), but no TnC. Together, these observations suggest that regulation of contraction in adult *S. mansoni* does not occur through the thin filaments.

Discussion

Schistosome Smooth Muscle Contains Striated Muscle Thick Filaments. The key, unexpected finding from this study is that schistosome smooth muscle is built using striated muscle-like thick filaments. The presence of dense bodies and the absence of striations in schistosome sections (Fig. 1) show that these animals contain only smooth muscle in their body wall, supporting a previous ultrastructural study (36). These results are consistent with confocal light microscopic observations, using fluorescent phalloidin to label actin filaments, which demonstrated a uniform and continuous longitudinal distribution of actin in all fibers of adult muscle, with

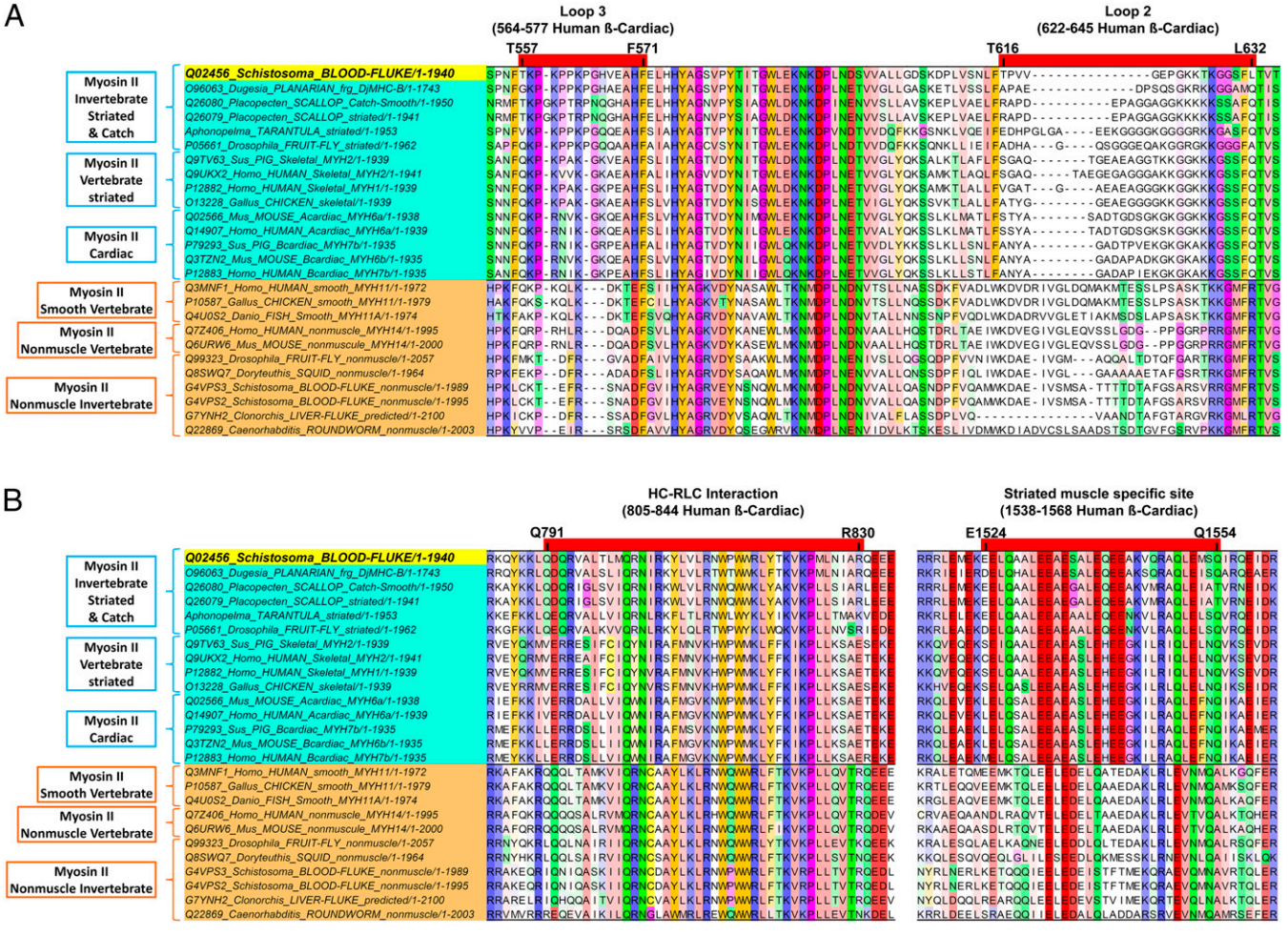

Fig. 5. Multiple sequence alignment of 26 MHC II sequences using the MUSCLE algorithm, comparing regions known to distinguish striated (cyan) from smooth/nonmuscle (tan) MHC II. The schistosome MHC II (yellow highlight) segregates with striated myosins and is quite distinct from smooth/nonmuscle myosins. Comparisons were made of actin-binding loops 2 and 3 of the motor domain (*A*), and the IQ motif of the regulatory domain and a striated muscle specific site in the tail (*B*). Besides the alignment of the whole MHC sequence, the S1 HC and the whole tail HC also were aligned independently, with the same grouping result. Sequences were retrieved from the UniProt sequence libraries.

Table 1. Sliding of native *S. mansoni* thin filaments and rabbit F-actin over tarantula thick filaments

	Schistosome thin filaments		Rabbit F-actin (51)	
	No Ca^{2+}	Ca^{2+}	No Ca^{2+}	Ca^{2+}
Tarantula thick filament	2.9 ± 1.3 (n = 380)	3.1 ± 1.3 (n = 567)	5.4 ± 2.1 (n = 574)	3.6 ± 1.3 (n = 321)

Sliding speed (μm/s) was measured using the in vitro motility assay, in the presence or absence of Ca^{2+}. Values shown are mean ± SD (n = number of measurements).

no appearance of striations (37); this was quite distinct from muscle fibers in the tail of the cercarial stage of the life cycle (the free-living stage that infects the mammalian host); these fibers were clearly recognized to be striated by the same technique (38). The organization of thick filaments, thin filaments, and dense bodies that we observed is similar to that previously described in other invertebrate smooth muscles (39). It is also similar to the smooth muscles of vertebrates (40), with the significant exception that the thick filaments in the schistosome are well preserved and very prominent [as in other invertebrates (39)], whereas in vertebrates they are labile and difficult to preserve (41).

Although the body musculature of the adult schistosome, both male and female, was clearly smooth muscle, we found that the thick filaments isolated from these muscles were identical to thick filaments from the striated muscles of other invertebrates (Fig. 2). This finding was supported by multiple sequence comparisons between the expressed schistosome MHC II and those of other species, which clearly show that schistosome MHC is a striated-type myosin (Figs. 4 and 5). Some other invertebrate muscles without cross-striations also have striated MHC II. Two striated MHC II isoforms were reported in muscles of the planarian (*Dugesia japonica*), which lack striations (8), whereas in *Caenorhabditis elegans*, having obliquely striated muscles (an intermediate form between smooth and cross-striated), four MHC II genes have been isolated, all classified as striated muscle-type (42). Finally, in the sea anemone *Nematostella vectensi* (33) and molluscan catch muscle (Fig. 5) with only smooth muscle, striated MHC II is strongly expressed. Together, these sequence data suggest that, in invertebrates, all types of muscle (smooth, cross-striated, and obliquely striated) can be built using only the striated MHC II sequence. Our thick filament EM observations and 3D reconstructions provide structural support for this conclusion, demonstrating that bipolar, helical thick filaments, indistinguishable from striated muscle thick filaments, are the structures present in schistosomal smooth muscle. In fact, during their life cycle, the schistosome develops—with striated-type MHC II sequence (the only type of muscle MHC gene reported)—both striated (cercaria tail) (43) and smooth (schistosomule and adult worm) muscle.

Schistosome Smooth Muscles Are Probably Regulated by Myosin Phosphorylation. Evolutionary studies based on both genome mining and biochemical data suggest that the thin filament protein, troponin, is a hallmark of striated muscle regulation in bilaterians (33, 44). By binding Ca^{2+}, troponin makes possible the rapid contractile response to changes in Ca^{2+} levels that characterizes movement in this animal group (9). Our motility studies suggest that the thin filaments of schistosome smooth muscle lack Ca^{2+}-sensitivity, consistent with the absence of the Ca^{2+}-sensitizing subunit of troponin (TnC) in the schistosome genome (29). It is possible that troponin functions in the striated muscles of the cercarial stage of the life cycle (possibly with a different Ca^{2+}-sensitizing component), where it may underlie rapid (20 Hz) movements of the tail (43, 45). Troponin is absent from the genomes of more primitive animals, including cnidarians (jellyfish and anemones), ctenophores (comb jellies), placozoans, and sponges (33). In these species, the presence of myosin light chain kinase (MLCK) suggests that regulation occurs via phosphorylation of the myosin regulatory light chain (RLC) (46), apparently the most ancient regulatory system in the Metazoa (33). In the absence of an intact troponin system, adult schistosome muscle is presumably also regulated by RLC phosphorylation; this is supported by the presence of a smooth muscle MLCK consensus phosphorylation site on the RLC (see below) and the presence of MLCK in the *S. mansoni* genome (29). This slow enzymatic mechanism of muscle activation is consistent with the leisurely, undulating motions exhibited by these lower invertebrates (e.g., jellyfish) and presumably could also suffice for the slow movements that we observe in live *S. mansoni* moving in artificial medium. Similarly, RLC phosphorylation underlies the slow response of vertebrate smooth muscles to activation (46–48). RLC phosphorylation also occurs in many striated muscles (e.g., mammals, spiders), where it functions—over an extended time frame—to modulate contractile force regulated primarily by the rapid on-off troponin switch (49).

In tarantula, the RLC contains a long N-terminal extension that incorporates sites for phosphorylation by both MLCK and protein kinase C (50), producing mono- or biphosphorylation (51). This long extension is unique to invertebrates and appears to be present in only two taxonomic groups, Ecdysozoa (Arthropoda) and Lophotrocozoa (Platyhelminthes and Annelids) (Fig. S2). Platyhelminthes are the only organisms of these groups with smooth muscle (52), suggesting that their smooth muscles could share a related myosin phosphorylation mechanism to that in the striated muscles. However, our analysis suggests that in the Platyhelminthes this is the primary mode of regulation, whereas with the other species it modulates the troponin regulatory mechanism (44). Analysis of the schistosome RLC suggests that it is a hybrid, exhibiting a long RLC N-terminal extension, as in tarantula striated muscle, but with a smooth muscle MLCK consensus sequence rather than the striated muscle MLCK sequence present in tarantula.

Schistosomes Provide New Insights into Muscle Evolution. Our results have broad implications for understanding how muscles are built and how they evolved. The schistosome thick filament reconstruction clearly demonstrates the presence of the interacting-heads motif in the off-state (Fig. 2*C*), providing further evidence that this highly conserved structure arose early in evolution as a means of inhibiting myosin II activity under relaxing conditions (22).

Table 2. Sliding of native tarantula thin filaments over tarantula or *S. mansoni* thick filaments

	Tarantula thin filaments	
Filament	No Ca^{2+}	Ca^{2+}
Tarantula thick filament (51)	No movement	9.8 ± 1.9 (n = 130)
Schistosome thick filament	No movement	9.3 ± 2.6 (n = 18)

Sliding speed (μm/s) was measured using the in vitro motility assay, in the presence or absence of Ca^{2+}. Values shown are mean ± SD (n = number of measurements).

This motif has now been demonstrated in striated muscle thick filaments of chelicerates (22–24), molluscs (53), vertebrates (54, 55), and here in the smooth muscle thick filaments of a Platyhelminth. Observation of the motif in single myosin molecules (in cases where it has not yet been demonstrated in thick filaments) extends this list to vertebrate smooth muscle (25, 56) and nonmuscle myosin (57), and to the most primitive animals with muscles, *Cnidaria* (sea anemones, jellyfish) (58).

Although the interacting-heads motif was not unexpected (given the number and diversity of species in which it had already been demonstrated), the finding that the structure of the schistosome thick filament was identical in every discernible detail to that in the striated muscle thick filaments of chelicerates (tarantula, scorpion, and *Limulus*) was a complete surprise. The similarity includes not only the interacting heads, but the filament diameter, the fourfold rotational symmetry, the coincidence of the helical repeats (43.5 nm in both species), and the organization of myosin tails into twelve, 4-nm-diameter subfilaments in the filament backbone (Fig. 2*D*). There are two aspects to this unexpected discovery: first, that the schistosome and chelicerates have essentially identical filament structures, even though they are evolutionarily quite separate; and second, that a filament with a striated muscle-type structure is found in a smooth muscle.

Chelicerate-like thick filaments in a Platyhelminth. The essentially identical thick filament structures in *S. mansoni* and chelicerates is puzzling and could be interpreted in two ways. Either Platyhelminthes are close evolutionary relatives of chelicerates (i.e., the filaments are homologous), or the structure is an example of convergent evolution. Convergent evolution appears to be less likely as an explanation because it normally refers to structures that are superficially similar but different in detail (59). However, we cannot exclude this possibility. The alternative explanation, that Platyhelminthes are close relatives of chelicerates, is also uncertain. In early evolutionary trees, based primarily on morphology, Platyhelminthes were considered to be one of the most primitive organisms and were placed near the base of the trunk (60), far from chelicerates. In more recent, molecular phylogenetic trees, based on protein (including MHC II) and ribosomal RNA sequence similarities (61), they are much closer to chelicerates (59, 60, 62), consistent with our structural findings. On the other hand, more closely related groups within the arthropods have different thick filament symmetries from chelicerates (63, 64), which would argue against the idea that a close evolutionary relationship between chelicerates and Platyhelminthes explains the similarity in their thick filaments. A third possibility is that the last common ancestor of arthropods and Platyhelminthes had the thick filament structure that we have described, and that this then changed to fulfill the specific functional needs of particular arthropod and other groups as they evolved, but was retained in the chelicerates and Platyhelminthes.

Striated muscle-like thick filaments in a smooth muscle. The organization of myosin in the schistosome thick filament is completely different from that in the only two other types of smooth muscle thick filament that have been examined in molecular detail. In vertebrate smooth muscle filaments, myosin molecules are organized in side-polar arrays that lack both helical symmetry and a central bare zone (11, 12), both key features of schistosome filaments. In addition, the MHC II sequence is of the smooth/nonmuscle type (27, 28), and the filaments are highly labile and readily dissociate (41, 65). This is in clear contrast to schistosome filaments, which we observed to be stable both as isolated filaments and in muscle sections, consistent with their construction from striated-type MHC II. Molluscan smooth muscles are characterized by giant thick filaments (up to 40 μm in length and 150 nm in diameter) (66–68). These filaments have a large core of paramyosin molecules in a paracrystalline array, and a thin surface layer of myosin molecules, which appear to have no direct geometric relationship to the underlying paramyosin (68). Thus, molluscan smooth muscle filaments are structurally quite different from any known striated muscle thick filament. Interestingly, however, their MHC II sequence is closely similar to that of their striated muscle myosin sequence (69), unlike the clear differences between vertebrate smooth and striated muscle myosins (Fig. 4). To our knowledge, no other smooth muscle thick filaments have been studied structurally at the molecular level. Thus, the schistosome employs a different strategy from that used in either vertebrates or molluscs in the construction of its smooth muscle: using a striated-type myosin assembled into a striated-type thick filament.

Conclusions

Our study shows that in schistosomes (and possibly other Platyhelminthes), nature takes a hybrid approach to building smooth muscle, making use of a striated muscle MHC and a hybrid, striated-smooth RLC, assembled into striated muscle-like thick filaments, which are combined with smooth muscle-like thin filaments in a smooth muscle architecture. The presence of striated MHC sequences in the smooth muscles of the planarian *D. japonica* (8) and the sea anemone *N. vectensis* (33) suggests that the same principle may pertain in other species. If so, then smooth and striated muscles in the invertebrates may have evolved using the same basic building blocks but in different organizations. It appears likely that the co-opting of nonmuscle-like myosin, and its assembly into side-polar filaments, may be a specialization unique to the smooth muscles of vertebrates. Our findings therefore challenge the paradigm (based on studies of vertebrates) that smooth and striated muscles always have distinctly different components. These findings also emphasize the fact that classification of muscle based simply on the presence or absence of striations only partially reflects its diversity in primitive invertebrate organisms (70). The principle of mixing and matching that nature uses to build different smooth muscles is also apparent in striated muscles, which appear to have evolved at least twice, using similar myosin and actin components, but different Z-line constituents (33).

Materials and Methods

Schistosomes. *S. mansoni* adult worms ["JL strain, Venezuela," maintained at the Instituto Venezolano de Investigaciones Científicas (IVIC) Trematodiasis Unit] were obtained by perfusion from the portal vein of golden hamsters infected with 500 cercariae (16). All procedures involving animals were performed according to the National Guidelines for Laboratory Animals established by the "Asociación Venezolana de Bioterios." The study protocol was approved by the Committee of Bioethics for Animals at IVIC under the reference no. 1415.

Schistosome Thick Filaments. *S. mansoni* relaxed thick filaments were isolated according to ref. 71, with some modifications. Six-thousand worms were permeabilized in 2-mL relaxing solution (100 mM NaCl, 3 mM $MgCl_2$, 1 mM EGTA, 5 mM Pipes, 1 mM NaN_3, 5 mM MgATP, pH 7.0) containing a protease inhibitor mixture (Sigma P-8465 plus aprotinin and leupeptin, a combination chosen as the most effective against the proteolytic enzymes in the gut and vomit of the parasite) and 0.1% (wt/vol) saponin for 6 h at 4 °C. The filaments were then washed overnight in relaxing solution at the same temperature, and homogenized twice for 2 s using a Sorvall Omni-mixer (Ivan Sorvall). The homogenate was centrifuged briefly (2,000 × *g* for 5 min) in a Thermo Sorvall Legend Micro 17R centrifuge to remove large debris, and the supernatant centrifuged for 20 min at 17,000 × *g*. For EM, the pellet containing thick and thin filaments was resuspended and blebbistatin was added to a final concentration of 10 μM. One drop of filament suspension was placed on a 400-mesh holey carbon grid coated with a thin layer of carbon which extended over the holes. The grid was negatively stained with 1% uranyl acetate (72).

Thin Sectioning. Worms, male or female, were fixed with 2.5% (vol/vol) glutaraldehyde and 4% (vol/vol) paraformaldehyde in 0.1 M sodium cacodylate buffer, pH 7.2, for 24 h, then washed twice in cacodylate buffer for 1 h. They were then cut into small pieces about 1- to 3-mm long, postfixed in 1% osmium tetroxide in 0.1 M cacodylate buffer for 1 h minimum, and washed overnight in cacodylate buffer, pH 7.2. The tissue pieces were stained in 1% aqueous uranyl acetate, pH 4.5, for 60 min and washed in water for 30 min.

Samples were dehydrated in a graded ethanol series and embedded in EPON. Ultrathin sections (60 nm) were cut on a diamond knife using a Leica UC7 ultra-microtome. Images were obtained on an FEI Tecnai Spirit BioTWIN 12 electron microscope at 80 kV using a Gatan Erlangshen ES1000W CCD camera.

Image Processing and 3D Reconstruction. For image processing, 263 electron micrographs of negatively stained *S. mansoni* thick filaments were acquired at 80 kV under low-dose conditions on a Philips CM120 electron microscope (FEI) with a pixel size of 0.57 nm, using a 2K × 2K CCD camera (F224HD, Tietz Video and Image Processing Systems). From these micrographs, 820 thick filament halves were selected and stored in SPIDER (73) format. Next, 131 × 131-pixel segments were cut from these filaments, corresponding to a window of 747 Å (~five 145 Å-spaced crowns of heads). Three-dimensional reconstruction was carried out by Iterative Helical Real Space Reconstruction (74) modified according to ref. 23. For each iteration of the reconstruction (30 cycles), filament segment projections were compared with different projections of the reference reconstruction as follows: seven 2.3-nm axial shifts, 2° intervals of rotation about the filament axis up to 90°, and 2° intervals of out-of-plane tilting from −10° to +10°. The total number of projections was therefore 7 × 45 × 11 = 3,465. For the final 19 cycles of the reconstruction, we used only the best-ordered 420 filament halves (those in which >30% of segments were found good enough to be used by the reconstruction script in the back projection in previous cycles). From ~17,000 segments, ~9,500 (56%) were included in the final reconstruction. This final 3D reconstruction was the average of the last 19 reconstructions between cycles 12 and 30. Its resolution, according to the 0.5 Fourier Shell Correlation criterion, was 2.3 nm.

Gel Electrophoresis. One-dimensional SDS/PAGE was carried out on 15% (wt/vol) gels, as described previously (75) using a Mini-Protean II electrophoresis chamber (Bio-Rad Laboratories). Schistosome filament homogenate components (50 μg per lane) were separated first at 50 V for 30 min and then at 150 V. For 2D-PAGE, 75 μg of protein from the filament homogenate was used. The homogenate proteins were solubilized in isolectric focusing rehydration buffer [8M Urea, 2M Thiourea, 4% (wt/vol) CHAPS, 0.0025% bromophenol buffer, 70 mM DTT, and 0.4 Biolyte 3–10 buffer (Bio-Rad #63–1113)]. The samples were loaded into 7-cm Immobilized pH Gradient (Bio-Rad) strips (in the pH ranges of 3–10 and 4–7). Isoelectric focusing was carried out according to ref. 76. The 1D or 2D gels were stained with Coomassie blue-R and destained with 25% (vol/vol) methanol, 10% (vol/vol) acetic acid.

Proteomic Analysis. Bands and spots from 1D or 2D SDS/PAGE gels were excised with a scalpel, carefully avoiding keratin contamination. Bands or spots were destained with 250 mM NH_4HCO_3/30% (vol/vol) acetonitrile for 10 min, washed with MilliQ water for 5 min, sliced into 1-mm^3 segments, dehydrated with 90% (vol/vol) acetonitrile, and dried for 5 min using a speed-vacuum centrifuge, all at room temperature. In-gel tryptic digestion (Promega, Sequencing Grade Modified) was carried out for 18 h at 37 °C. Peptides were extracted (1% formic acid) and the supernatant loaded through a ZipTip C18 microcolumn (Millipore). Samples were eluted with 60% (vol/vol) acetonitrile/1% formic acid and mixed with saturated matrix solution [α-cyano-4-hydroxycinnamic acid in 50% (vol/vol) acetonitrile/0.1% TFA] in a 1:1 ratio. MALDI-TOF spectra were collected from spots and analyzed on an Autoflex III Smartbeam (Bruker Daltonics). External calibration was performed with a commercial peptide mixture (Peptide Calibration Standard, Bruker Daltonics). The analysis was conducted using 200 shots of MS and 500 shots of MS/MS. The list of peptides and fragment mass values generated by the mass spectrometer for each spot was submitted to a MS/MS ion search using MASCOT (Matrix Science). The parameters used were: allowance of one tryptic missed cleavage, peptide mass tolerance of ±0.6 Da, fragment mass tolerance ±0.3 Da, peptide charge +1, fixed modification: Propionamide (C), variable modification of oxidation (M), Deamidated (NQ). Only ions with individual scores above those specified by MASCOT as indicating identity or extensive homology ($P < 0.05$) were considered for protein identification.

In Vitro Motility Assay. To obtain *S. mansoni* or tarantula thin filaments, the supernatant from the thick filament preparations, after 20 min centrifugation, was centrifuged again at 17,000 × *g* for 1 h, the pellet discarded, and the supernatant containing the thin filaments collected. Activity of thick filaments from *S. mansoni* and *Avicularia avicularia* (tarantula, control) homogenates was tested by measuring the motility that they produced using purified rabbit F-actin and *A. avicularia* or *S. mansoni* thin filaments made visible by labeling with fluorescently tagged phalloidin. Fifteen microliters of relaxed filament homogenate (schistosome or tarantula) was introduced into the motility chamber and flushed with a washing solution (25 mM NaCl, 3 mM $MgCl_2$, 1 mM EGTA, 3 mM NaN_3, 1 mM DTT, 5 mM Pipes, 25 mM Imidazol, 3 mg/mL BSA, 1 mM Mg.ATP; pH 7.5). Next, 500 μL of tarantula or *S. mansoni* thin filaments or rabbit F-actin in relaxing solution were fluorescently labeled with 2.5 μL rhodamine/phalloidin (Sigma-Aldrich, P-1951) and a 15-μL aliquot was added to the chamber, followed by a 60-μL aliquot of activating solution (relaxing solution containing 1 μM free Ca^{2+}; pCa 6.0) for thin filaments. Movement of the fluorescently labeled filaments was tracked according to (51). This in vitro motility set-up enabled real-time image acquisition and analysis, speed calculations, and statistical analysis of tracked filaments.

Bioinformatics Analysis. JalView (77) (v2.8) was used to analyze sequences retrieved from UniProt libraries (www.uniprot.org/). Only complete sequences with evidence at transcriptional or protein level were used for the analysis. The sequences were aligned with MUSCLE (78) (v3.8.31) using default parameters; the percent identity average distance tree was calculated and the sequences were ordered accordingly. SCORER 2.0 (coiledcoils.chm.bris.ac.uk/Scorer/) was used to determine the number of skip residues in the *S. mansoni* MHC (UniProt Q02456).

Accession Numbers. The *S. mansoni* negatively stained thick filament 3D map has been deposited into the Electron Microscopy Data Bank (EMD-6370), and the atomic coordinates of the rigid docked model of myosin II interacting heads (PDB ID code 3DTP) have been deposited into the Research Collaboratory for Structural Bioinformatics as PDB ID code 3JAX.

ACKNOWLEDGMENTS. We thank Dr. Carolyn Cohen and Dr. Rhea Levine (deceased) for their enthusiastic support at the beginning of this project; Dr. Oscar Noya for his support and discussion; Dr. Jesús Mavárez for his help with understanding the evolutionary position of Platyhelminthes; María José Martelo, Maristela Granados, and Dr. Italo Cesari for their initial help with this work (79); Mónica Rincón and Dr. Eva Vonasek (Unidad de Proteómica, Centro de Biología Estructural, Instituto Venezolano de Investigaciones Científicas) for their help with MS experiments; and the Instituto Venezolano de Investigaciones Científicas Trematodiasis Unit as the source of the *Schistosoma mansoni* JL strain. This work was supported by National Institutes of Health Grants R01 AR034711 (to R.C.) and P01 HL059408 (to D. Warshaw), and a grant from the Howard Hughes Medical Institute (to R.P.).

1. Craig R, Padrón R (2004) Molecular structure of the sarcomere. *Myology*, eds Engel AG, Franzini-Armstrong C (McGraw-Hill, New York), pp 129–166.
2. Clark KA, McElhinny AS, Beckerle MC, Gregorio CC (2002) Striated muscle cytoarchitecture: An intricate web of form and function. *Annu Rev Cell Dev Biol* 18(1):637–706.
3. Gabella G (1984) Structural apparatus for force transmission in smooth muscles. *Physiol Rev* 64(2):455–477.
4. Prosser CL (1980) Evolution and diversity of nonstriated muscles. *Handbook of Physiology: Vascular Smooth Muscle*, eds Bohr DF, Somlyo AP, Sparks HV (American Physiological Society, Bethesda, MD), pp 635–670.
5. Royuela M, Fraile B, Arenas MI, Paniagua R (2000) Characterization of several invertebrate muscle cell types: A comparison with vertebrate muscles. *Microsc Res Tech* 48(2):107–115.
6. Craig R, Woodhead JL (2006) Structure and function of myosin filaments. *Curr Opin Struct Biol* 16(2):204–212.
7. Schuchert P, Reber-Müller S, Schmid V (1993) Life stage specific expression of a myosin heavy chain in the hydrozoan *Podocoryne carnea*. *Differentiation* 54(1):11–18.
8. Kobayashi C, et al. (1998) Identification of two distinct muscles in the planarian *Dugesia japonica* by their expression of myosin heavy chain genes. *Zoolog Sci* 15(6):861–869.
9. Gordon AM, Homsher E, Regnier M (2000) Regulation of contraction in striated muscle. *Physiol Rev* 80(2):853–924.
10. Hirano K, Derkach DN, Hirano M, Nishimura J, Kanaide H (2003) Protein kinase network in the regulation of phosphorylation and dephosphorylation of smooth muscle myosin light chain. *Mol Cell Biochem* 248(1-2):105–114.
11. Craig R, Megerman J (1977) Assembly of smooth muscle myosin into side-polar filaments. *J Cell Biol* 75(3):990–996.
12. Xu JQ, Harder BA, Uman P, Craig R (1996) Myosin filament structure in vertebrate smooth muscle. *J Cell Biol* 134(1):53–66.
13. Butler TM, Siegman MJ (2010) Mechanism of catch force: Tethering of thick and thin filaments by twitchin. *J Biomed Biotechnol* 2010:725207.
14. Gryseels B, Polman K, Clerinx J, Kestens L (2006) Human schistosomiasis. *Lancet* 368(9541):1106–1118.
15. Gnanasekar M, Salunkhe AM, Mallia AK, He YX, Kalyanasundaram R (2009) Praziquantel affects the regulatory myosin light chain of *Schistosoma mansoni*. *Antimicrob Agents Chemother* 53(3):1054–1060.

16. Sulbarán G, Noya O, Brito B, Ballén DE, Cesari IM (2013) Immunoprotection of mice against *Schistosomiasis mansoni* using solubilized membrane antigens. *PLoS Negl Trop Dis* 7(6):e2254.
17. Soisson LM, et al. (1992) Induction of protective immunity in mice using a 62-kDa recombinant fragment of a *Schistosoma mansoni* surface antigen. *J Immunol* 149(11): 3612–3620.
18. Matsumoto Y, et al. (1988) Paramyosin and actin in schistosomal teguments. *Nature* 333(6168):76–78.
19. Crowther RA, Padrón R, Craig R (1985) Arrangement of the heads of myosin in relaxed thick filaments from tarantula muscle. *J Mol Biol* 184(3):429–439.
20. Kensler RW, Levine RJ, Stewart M (1985) Electron microscopic and optical diffraction analysis of the structure of scorpion muscle thick filaments. *J Cell Biol* 101(2):395–401.
21. Stewart M, Kensler RW, Levine RJ (1981) Structure of *Limulus telson* muscle thick filaments. *J Mol Biol* 153(3):781–790.
22. Woodhead JL, et al. (2005) Atomic model of a myosin filament in the relaxed state. *Nature* 436(7054):1195–1199.
23. Pinto A, Sánchez F, Alamo L, Padrón R (2012) The myosin interacting-heads motif is present in the relaxed thick filament of the striated muscle of scorpion. *J Struct Biol* 180(3):469–478.
24. Zhao FQ, Craig R, Woodhead JL (2009) Head-head interaction characterizes the relaxed state of *Limulus* muscle myosin filaments. *J Mol Biol* 385(2):423–431.
25. Wendt T, Taylor D, Trybus KM, Taylor K (2001) Three-dimensional image reconstruction of dephosphorylated smooth muscle heavy meromyosin reveals asymmetry in the interaction between myosin heads and placement of subfragment 2. *Proc Natl Acad Sci USA* 98(8):4361–4366.
26. Hooper SL, Thuma JB (2005) Invertebrate muscles: Muscle specific genes and proteins. *Physiol Rev* 85(3):1001–1060.
27. Cheney RE, Riley MA, Mooseker MS (1993) Phylogenetic analysis of the myosin superfamily. *Cell Motil Cytoskeleton* 24(4):215–223.
28. Goodson HV, Spudich JA (1993) Molecular evolution of the myosin family: Relationships derived from comparisons of amino acid sequences. *Proc Natl Acad Sci USA* 90(2):659–663.
29. Berriman M, et al. (2009) The genome of the blood fluke *Schistosoma mansoni*. *Nature* 460(7253):352–358.
30. Rovner AS, Freyzon Y, Trybus KM (1995) Chimeric substitutions of the actin-binding loop activate dephosphorylated but not phosphorylated smooth muscle heavy meromyosin. *J Biol Chem* 270(51):30260–30263.
31. Trybus KM, Naroditskaya V, Sweeney HL (1998) The light chain-binding domain of the smooth muscle myosin heavy chain is not the only determinant of regulation. *J Biol Chem* 273(29):18423–18428.
32. Offer G (1990) Skip residues correlate with bends in the myosin tail. *J Mol Biol* 216(2): 213–218.
33. Steinmetz PR, et al. (2012) Independent evolution of striated muscles in cnidarians and bilaterians. *Nature* 487(7406):231–234.
34. Straussman R, Squire JM, Ben-Ya'acov A, Ravid S (2005) Skip residues and charge interactions in myosin II coiled-coils: Implications for molecular packing. *J Mol Biol* 353(3):613–628.
35. Craig R, Lehman W (2001) Crossbridge and tropomyosin positions observed in native, interacting thick and thin filaments. *J Mol Biol* 311(5):1027–1036.
36. Silk MH, Spence IM (1969) Ultrastructural studies of the blood fluke—*Schistosoma mansoni*. II. The musculature. *S Afr J Med Sci* 34(1):11–20.
37. Mair GR, Maule AG, Day TA, Halton DW (2000) A confocal microscopical study of the musculature of adult *Schistosoma mansoni*. *Parasitology* 121(2):163–170.
38. Collins JJ, 3rd, King RS, Cogswell A, Williams DL, Newmark PA (2011) An atlas for *Schistosoma mansoni* organs and life-cycle stages using cell type-specific markers and confocal microscopy. *PLoS Negl Trop Dis* 5(3):e1009.
39. Paniagua R, Royuela M, García-Anchuelo RM, Fraile B (1996) Ultrastructure of invertebrate muscle cell types. *Histol Histopathol* 11(1):181–201.
40. Ashton FT, Somlyo AV, Somlyo AP (1975) The contractile apparatus of vascular smooth muscle: Intermediate high voltage stereo electron microscopy. *J Mol Biol* 98(1):17–29.
41. Shoenberg CF (1973) The influence of temperature on the thick filaments of vertebrate smooth muscle. *Philos Trans R Soc Lond B Biol Sci* 265(867):197–202.
42. Dibb NJ, Maruyama IN, Krause M, Karn J (1989) Sequence analysis of the complete *Caenorhabditis elegans* myosin heavy chain gene family. *J Mol Biol* 205(3):603–613.
43. Nuttman CJ (1974) The fine structure and organization of the tail musculature of the cercaria of *Schistosoma mansoni*. *Parasitology* 68(2):147–154.
44. Lehman W, Szent-Györgyi AG (1975) Regulation of muscular contraction. Distribution of actin control and myosin control in the animal kingdom. *J Gen Physiol* 66(1):1–30.
45. Graefe G, Hohorst W, Dräger H (1967) Forked tail of the cercaria of *Schistosoma mansoni*—A rowing device. *Nature* 215(5097):207–208.
46. Sellers JR (1999) *Myosins* (Oxford Univ Press, Oxford), 2nd Ed.
47. Horiuti K, Somlyo AV, Goldman YE, Somlyo AP (1989) Kinetics of contraction initiated by flash photolysis of caged adenosine triphosphate in tonic and phasic smooth muscles. *J Gen Physiol* 94(4):769–781.
48. Zimmermann B, Somlyo AV, Ellis-Davies GC, Kaplan JH, Somlyo AP (1995) Kinetics of prephosphorylation reactions and myosin light chain phosphorylation in smooth muscle. Flash photolysis studies with caged calcium and caged ATP. *J Biol Chem* 270(41):23966–23974.
49. Sweeney HL, Bowman BF, Stull JT (1993) Myosin light chain phosphorylation in vertebrate striated muscle: Regulation and function. *Am J Physiol* 264(5):C1085–C1095.
50. Alamo L, et al. (2008) Three-dimensional reconstruction of tarantula myosin filaments suggests how phosphorylation may regulate myosin activity. *J Mol Biol* 384(4): 780–797.
51. Brito R, et al. (2011) A molecular model of phosphorylation-based activation and potentiation of tarantula muscle thick filaments. *J Mol Biol* 414(1):44–61.
52. Hooper SL, Hobbs KH, Thuma JB (2008) Invertebrate muscles: Thin and thick filament structure; molecular basis of contraction and its regulation, catch and asynchronous muscle. *Prog Neurobiol* 86(2):72–127.
53. Woodhead JL, Zhao FQ, Craig R (2013) Structural basis of the relaxed state of a Ca2+ -regulated myosin filament and its evolutionary implications. *Proc Natl Acad Sci USA* 110(21):8561–8566.
54. Zoghbi ME, Woodhead JL, Moss RL, Craig R (2008) Three-dimensional structure of vertebrate cardiac muscle myosin filaments. *Proc Natl Acad Sci USA* 105(7):2386–2390.
55. Al-Khayat HA, Kensler RW, Squire JM, Marston SB, Morris EP (2013) Atomic model of the human cardiac muscle myosin filament. *Proc Natl Acad Sci USA* 110(1):318–323.
56. Burgess SA, et al. (2007) Structures of smooth muscle myosin and heavy meromyosin in the folded, shutdown state. *J Mol Biol* 372(5):1165–1178.
57. Jung HS, Komatsu S, Ikebe M, Craig R (2008) Head-head and head-tail interaction: A general mechanism for switching off myosin II activity in cells. *Mol Biol Cell* 19(8): 3234–3242.
58. Sulbarán G, et al. (2015) The inhibited, interacting-heads motif characterizes myosin II from the earliest animals with muscle. *Biophys J* 108(2):301a.
59. Gordon MS, Notar JC (2015) Can systems biology help to separate evolutionary analogies (convergent homoplasies) from homologies? *Prog Biophys Mol Biol* 117(1): 19–29.
60. Valentine JW (1989) Bilaterians of the Precambrian-Cambrian transition and the annelid-arthropod relationship. *Proc Natl Acad Sci USA* 86(7):2272–2275.
61. Yang Z, Rannala B (2012) Molecular phylogenetics: Principles and practice. *Nat Rev Genet* 13(5):303–314.
62. Ruiz-Trillo I, et al. (2002) A phylogenetic analysis of myosin heavy chain type II sequences corroborates that Acoela and Nemertodermatida are basal bilaterians. *Proc Natl Acad Sci USA* 99(17):11246–11251.
63. Wray JS (1979) Structure of the backbone in myosin filaments of muscle. *Nature* 277(5691):37–40.
64. Miller A, Tregear RT (1972) Structure of insect fibrillar flight muscle in the presence and absence of ATP. *J Mol Biol* 70(1):85–104.
65. Suzuki H, Onishi H, Takahashi K, Watanabe S (1978) Structure and function of chicken gizzard myosin. *J Biochem* 84(6):1529–1542.
66. Levine RJ, Elfvin M, Dewey MM, Walcott B (1976) Paramyosin in invertebrate muscles. II. Content in relation to structure and function. *J Cell Biol* 71(1):273–279.
67. Chantler PD (2006) Scallop adductor muscles: Structure and function. *Scallops: Biology, Ecology and Aquaculture*, eds Shumway SE, Parsons GJ (Elsevier, Amsterdam), pp 231–320.
68. Castellani L, Vibert P, Cohen C (1983) Structure of myosin/paramyosin filaments from a molluscan smooth muscle. *J Mol Biol* 167(4):853–872.
69. Nyitray L, Jancsó A, Ochiai Y, Gráf L, Szent-Györgyi AG (1994) Scallop striated and smooth muscle myosin heavy-chain isoforms are produced by alternative RNA splicing from a single gene. *Proc Natl Acad Sci USA* 91(26):12686–12690.
70. Dayraud C, et al. (2012) Independent specialisation of myosin II paralogues in muscle vs. non-muscle functions during early animal evolution: A ctenophore perspective. *BMC Evol Biol* 12(1):107.
71. Craig R, Padrón R, Kendrick-Jones J (1987) Structural changes accompanying phosphorylation of tarantula muscle myosin filaments. *J Cell Biol* 105(3):1319–1327.
72. Craig R (2012) Isolation, electron microscopy and 3D reconstruction of invertebrate muscle myofilaments. *Methods* 56(1):33–43.
73. Frank J, et al. (1996) SPIDER and WEB: Processing and visualization of images in 3D electron microscopy and related fields. *J Struct Biol* 116(1):190–199.
74. Egelman EH (2000) A robust algorithm for the reconstruction of helical filaments using single-particle methods. *Ultramicroscopy* 85(4):225–234.
75. Laemmli UK (1970) Cleavage of structural proteins during the assembly of the head of bacteriophage T4. *Nature* 227(5259):680–685.
76. Ludolf F, et al. (2014) Serological screening of the *Schistosoma mansoni* adult worm proteome. *PLoS Negl Trop Dis* 8(3):e2745.
77. Waterhouse AM, Procter JB, Martin DM, Clamp M, Barton GJ (2009) Jalview version 2 —A multiple sequence alignment editor and analysis workbench. *Bioinformatics* 25(9):1189–1191.
78. Edgar RC (2004) MUSCLE: Multiple sequence alignment with high accuracy and high throughput. *Nucleic Acids Res* 32(5):1792–1797.
79. Martelo MJ, Granados M, Cesari I, Padrón R (1987) Estudio por microscopía electrónica de los filamentos gruesos aislados de músculo de *Schistosoma mansoni*. *Acta Cient Venez* 38(1):227.
80. Weston D, Schmitz J, Kemp WM, Kunz W (1993) Cloning and sequencing of a complete myosin heavy chain cDNA from *Schistosoma mansoni*. *Mol Biochem Parasitol* 58(1):161–164.